

Numerical Analysis of Combustion Dynamics for Single-stage entrained flow gasifier

Bilal Hussain¹, Hafiz Waqar Azmat², Muhammad Usman Bashir³, Muhammad Umer⁴,

1. Shanghai Jiao Tong University, Minhang Shanghai

2. University of Wollongong Australia

3. HITEC University, Taxila Pakistan

4. Beijing University of Chemical Technology, Beijing

Abstract

Clean coal technology (CCT) is an environmentally friendly technology for producing syngas. The gasification process is part of CCT for producing the syngas. The numerical simulation of the gasification process is much more economical compared to the experimental study. So, it is beneficial for calculating syngas composition and helping to improve the gasification process. In the present research, the single-stage entrained gasifier is considered for the syngas composition analysis. In the study, the volatile break-up was estimated by the finite volume method. The reaction rates are analyzed using the Finite rate dissipation reaction model. The syngas composition and the exit temperature result of simulation follow behavior reported in the literature.

Keywords: Single-stage entrained flow gasifier; coal gasification; Computational fluid dynamics; Clean coal technology

Introduction:

Energy is an integral part of human life processes such as electrical power generation, transportation and industrial manufacturing processes. Fossil fuel is the primary source for the generation of energy. Energy generation from fossil fuel results in releasing of CO₂ into the atmosphere. The CO₂ in the atmosphere giving rise to global warming and other severe threats to our environment. The concentration of CO₂ is gradually increasing from 280ppm to 400ppm and is expected to cross 750ppm by 2100 [1]. It is unable to meet energy demand and unable to replace the use of fossil fuel altogether. There is a need for other processes to make safe and efficient use of fossil fuel with less environmental pollution. Coal gasification is an alternate approach for the conversion of coal into a more useful energy source. There are three gasifier types: fixed bed, fluidized bed, and entrained flow gasifier are commercially available for coal gasification [2]. The entrained flow coal gasifier is a favorable choice due to high carbon conversion with low tar production at a high operating temperature [3]. The entrained flow gasifier can process different coal feedstocks, which attracts for their commercial application. It produces the syngas consisting of the mixture of H₂, CO, CO₂, and H₂O with a small number of contaminants separated from the product gas at the downstream side [4].

Coal gasification with entrained flow gasifier is a complex process involving the reaction between the turbulent multiphase flow of solid (fine coal particles) and gas phase (the oxidant), which is highly influenced by the thermodynamics and hydrodynamics of the reacting flow [5]. The air, oxygen-enriched air, pure oxygen, and steam are extensively used as an oxidant for coal gasification [6]. The product with a high calorific value can be obtained with oxygen as an oxidant, unlike air resulting in a lower calorific value. Firstly, during the coal gasification process, the coal's moisture content is released in the drying step. The thermal decomposition of coal takes place and subsequently, the reaction between volatile matter and O₂ occurs in the flame zone. Char oxidation occurs with O₂ and gasification agents such as CO₂ and H₂O to produce high CO and H₂ [7]. Radial

mass transport of molten ash for deposition at the wall's internal surface while liquid slag travels downward under the influence of gravity.

Numerical and computational methods are cost-effective and feasible alternatives to the experimental setup for designing, retrofitting, and optimizing entrained flow gasifiers [8]. Different numerical and computational approaches have received considerable attention to understanding the reacting flow in entrained flow gasifier. Many researchers adopted computational fluid dynamic tools incorporating sub-models for addressing various physical and chemical processes taking place during coal gasification. Shahabuddin M et al. analyzed the effect of different reactions at a temperature above 1000°C on the gasification process. He reported that almost 12 percent of carbon conversion occurs more during steam gasification than CO₂ gasification [9]. Jinliang Ma et al. [10] developed CFD model for single and two-stage entrained flow gasifier coupled sub-models for moisture vaporization, coal devolatilization, and gas-phase reaction kinetics. Neerav Abani et al. [11] has done large-eddy simulations of entrained flow gasifier that account unsteady flow structure inside the gasifier. Roberts D.G et al. [5] has developed the steady-state gasification model for entrained flow gasifier with improved reaction kinetics. G.L. Tufano et al. [12] studied the ignition delay in coal gasification by using resolved laminar flow simulation approach with improved reaction kinetics.

A shorter ignition delay time was observed with enhanced oxygen level. Lijun Wang et al. [13] found that the optimized value O₂/C ratio is 0.8 for the maximum yield of syngas. Zhikai Cao et al. [14] studied the nozzle effect on the product composition using the CFD model. The optimal bias angle is 5.0*(π/180) rad for entrained flow gasifier under various operating conditions. Kai Dong et al. [4] developed a model for entrained flow gasifiers in Aspen Plus. The model consists of different unit operations for each gasification step. Furkan et al. uses Turkish lignite as fuel in the entrained flow gasifier model study using the Aspen Plus for sensitivity and syngas analysis [15]. Figure 1 shows the mesh of a single entrained flow gasifier. The mesh minimum orthogonal quality is 9.998*10⁻¹, the volume is 5m³. minimum and maximum face areas are 1.7857*10⁻² and 3.104225*10⁻¹, respectively.

<https://doi.org/10.24949/njes.v13i2.634>



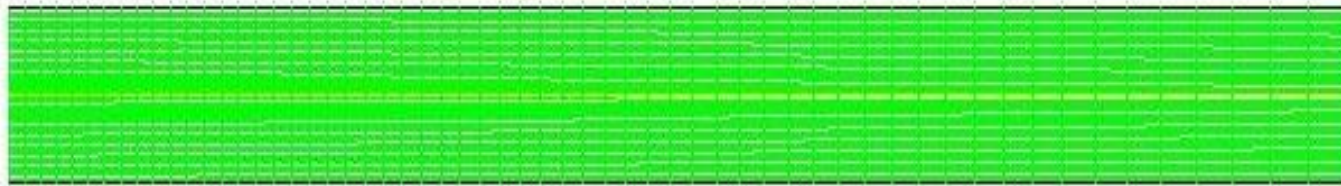


Figure 1 Mesh of single entrained flow gasifier

Table 1: Reactions

S.NO	Reactions	A	Ea $\times e^{+08}$ (J/Kmol)	References
R1	$vol \rightarrow aCo + bH_2 + cCH_4 + dH_2O + eH_2S + fO_2 + gN_2 + hTar$	2.119e ⁺¹¹	2.027	[16]
R2	Char Combustion $C < S > + 0.5O_2 \rightarrow CO$	300	1.3	[17]
R3	CO ₂ Gasification $C < S > + CO_2 \rightarrow 2CO$	2244	2.2	[17]
R4	H ₂ Gasification $C < S > + H_2 \rightarrow CH_4$	1.62	1.5	[17]
R5	H ₂ O Gasification $C < S > + H_2O \rightarrow CO + H_2$	42.5	1.42	[17]
R6	Methane Oxidation $CH_4 + 1.5O_2 \rightarrow CO + H_2O$	5.012e ⁺¹¹	2	[16]
R7	Steam methane reforming $CH_4 + H_2O - CO + 3H_2$	5.92 e ⁺⁰⁸	2.09	[18]
R8	CO oxidation $CO + 0.5O_2 \rightarrow CO_2$	2.239 e ⁺¹²	1.7	[16]
R9	The forward water-gas shift reaction $CO + H_2O \rightarrow CO_2 + H_2$	2.35 e ⁺¹⁰	2.88	[16]
R10	Reverse water-gas shift reaction $CO_2 + H_2 \rightarrow CO + H_2O$	1.785e ⁺¹²	3.26	[16]
R11	Hydrogen Oxidation $H_2 + 0.5O_2 \rightarrow H_2O$	9.87e ⁺⁸	0.31	[16]
R12	Reverse Hydrogen Oxidation $H_2O \rightarrow 0.5O_2 + H_2$	2.06 e ⁺¹¹	2.72	[16]
R13	Tar Oxidation $Tar + O_2 \rightarrow CO$	1e ⁺¹⁵	1	[19]

The coal's molecular structure is very complex and greatly varies with different coal types [20]. The studies on numerical simulation of entrained flow gasifier are done using the ANSYS FLUENT @ [21] for analyzing the composition of syngas using the coal as feed. The reactions applied for the simulation are given in Table 1. The operating conditions and coal properties are explained in Table 2 and Table 3. The model considers the detailed kinetics of thermal decomposition of volatile matters and their subsequent conversion. According to the literature reported previously, the product composition and temperature predicted from the present model show the trend.

Table 2: Operating and Boundary conditions

Operating and Boundary Parameters	Values
Operating Pressure	2.7 MPa
Inlet temperature all levels	521 K
Oxygen Velocity inlet 1	25m/sec
Oxygen Velocity inlet 2	100m/sec
Coal feed flow rate	0.25 kg/sec

Table 3: Coal properties for simulations

Proximate Analysis	Weight %
Fixed Carbon	50
Volatile	30
Moisture	10
Ash	10
Ultimate Analysis (DAF)	
Carbon	85
Hydrogen	10
Oxygen	4
Nitrogen	1
HHV	24.0MJ/Kg

Mathematical Model

Mass conservation equation is

$$\nabla \cdot (\rho \vec{v}) = S_m \quad (1)$$

Conservation of momentum equation is:

$$\nabla \cdot (\rho \vec{v} \vec{v}) = -\nabla p + \nabla \cdot (\vec{\tau}) + \rho \vec{g} + \vec{F} \quad (2)$$

Where p , τ , ρg and F shows the static pressure, stress tensor, gravitational and external body forces, respectively

The stress tensor can be calculated as

$$\vec{\tau} = \mu \left[(\nabla \vec{v} + \nabla \vec{v}^T) - \frac{2}{3} \nabla \cdot \vec{v} I \right] \quad (3)$$

The μ and I denote the molecular viscosity and unit tensor,

The conservation of energy is:

$$\frac{\partial}{\partial x_i} (\rho \bar{u}_i h) = \frac{\partial}{\partial x_i} \left(K \frac{\partial T}{\partial x_i} \right) + S_{ph} \quad (4)$$

The k - ε transport equation was used for the turbulence model. The different parameters such as kinetic energy, dissipation rate, turbulent Prandtl number and eddy viscosity are calculated from the following equations.

$$\frac{\partial}{\partial x_i} (\rho k u_i) = \frac{\partial}{\partial x_j} \left[\left(\mu + \frac{\mu_t}{\sigma_k} \right) \frac{\partial k}{\partial x_j} \right] + G_k - \rho \varepsilon \quad (5)$$

And

$$\frac{\partial}{\partial x_i} (\rho \varepsilon u_i) = \frac{\partial}{\partial x_j} \left[\left(\mu + \frac{\mu_t}{\sigma_\varepsilon} \right) \frac{\partial \varepsilon}{\partial x_j} \right] + C_{1\varepsilon} \frac{\varepsilon}{k} G_k - C_{2\varepsilon} \rho \frac{\varepsilon^2}{k} \quad (6)$$

$$\mu_t = \rho C_\mu \frac{k^2}{\varepsilon} \quad (7)$$

The constants values are $C_{1\varepsilon} = 1.44$, $C_{2\varepsilon} = 1.92$, $C_\mu = 0.09$, $\sigma_\varepsilon = 1.3$, $\sigma_k = 1.0$ [22]

The rate models for the computation of the coal particles devolatilization is as below. The constants values are $A_1 =$

2×10^5 , $A_2 = 1.3 \times 10^7$, $E_1 = 1.046 \times 10^8$ J/kg mol, and $E_2 = 1.67 \times 10^8$ J/kg mol.

$$R_1 = A_1 e^{-(E_1/RT_p)} \quad (8)$$

$$R_2 = A_2 e^{-(E_2/RT_p)} \quad (9)$$

The particle surface relations are heterogeneous reactions and the carbon depletion rate is due to the surface reactions. The relationships are given in equations (10,11,12) [23]. The endothermic reaction rate \bar{R}_k (kg/sec) for particle surface depletion is calculated from equation (8).

$$\bar{R}_k = A_p \eta_k Y_{carbon} \bar{R}_k \quad (10)$$

$$\bar{R}_k = k_{kin,k} \left(p_{i,k} - \frac{\bar{R}_k}{D_k} \right)^{N_k} \quad (11)$$

$$k_{kin} = A_f \exp^{-(E_\infty/RT_p)} \quad (12)$$

During devolatilization, the particle temperature change due to the char surface reaction with different chemicals such as oxygen, carbon dioxide, and water occurs, and heat balance is calculated from equation (14) [24].

$$m_p C_p \frac{dT_p}{dt} = h A_p (T - T_p) + \frac{dm_p}{dt} L + A_p \varepsilon_p \sigma (\theta_R^4 - T_p^4) \quad (13)$$

$$m_p C_p \frac{dT_p}{dt} = h A_p (T - T_p) + f_h \left(\frac{dm_p}{dt} \right) \Delta H + A_p \varepsilon_p \sigma (\theta_R^4 - T_p^4) \quad (14)$$

The eddy-dissipation rate equations are as follows. The mass fraction is Y_R and Y_P . Magnussen constant, molecular weight, and subscripts for reactant and product are A and B , M and R , P , respectively.

$$R_{i,r} = \min \left(R_{i,r}^{(R)}, R_{i,r}^{(P)} \right) \quad (15)$$

$$R_{i,r}^{(R)} = v'_{i,r} M_i A \rho \frac{\varepsilon}{k} \left(\frac{Y_R}{v'_{r,M_R}} \right) \quad (16)$$

$$R_{i,r}^{(P)} = v''_{i,r} M_i A B \frac{\varepsilon}{k} \left(\frac{\sum_j P Y_P}{\sum_j v''_{j,r} M_j} \right) \quad (17)$$

The discrete ordinate radiation model is for the radiative heat transfer.

$$\frac{dI_{rad}(\vec{r}, \vec{s})}{ds} = (a + a_p + \sigma_p) I_{rad}(\vec{r}, \vec{s}) + E_p + a \phi^2 \frac{\sigma T^4}{\pi} + \frac{\sigma_s}{4\pi} \int_0^{4\pi} I_{rad}(\vec{r}, \vec{s}) \Phi(\vec{s}, \vec{s}) d\Omega \quad (18)$$

Figure 2 shows the flow chart of the simulation setup following this study.

Result and discussion

Figures 3-6 show the contours of mass fractions of carbon monoxide, hydrogen, water, carbon dioxide, oxygen. The results show that in single-stage gasifiers, where the mass fraction of carbon dioxide is high, carbon monoxide is low. Still, along the length of carbon monoxide and water's char

reactions, the mass fraction of carbon dioxide is increased and carbon dioxide is decreased.

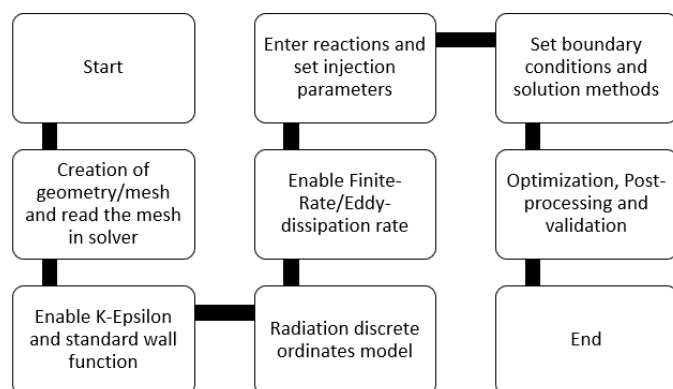


Figure 2 Flow chart of the simulation setup

The oxygen is the oxidizing agent, so the mass fraction of oxygen is high in the injection points. Still, due to combustion reactions, oxygen is utilized to form carbon dioxide and water. Still, after that mass fraction of oxygen is decreases, so in the presence of limited oxygen, the endothermic reactions occur, and hydrogen production increases.

Figures 7-8 show the velocity and temperature profile. At the injection point of the air, the velocity is more, but it decreases when the reactions occur along the length. From the temperature profile, it is observed that almost exothermic reactions occur almost at the center of the reactor. In that region, the temperature is high along the length. The temperature starts to decrease due to endothermic reactions. Figure 9 shows the temperature profile in the reactor. Figure 10 shows particles' residence time and points out that the particles' residence time is almost 0.17 seconds in the reactor, during which all the reactions occur

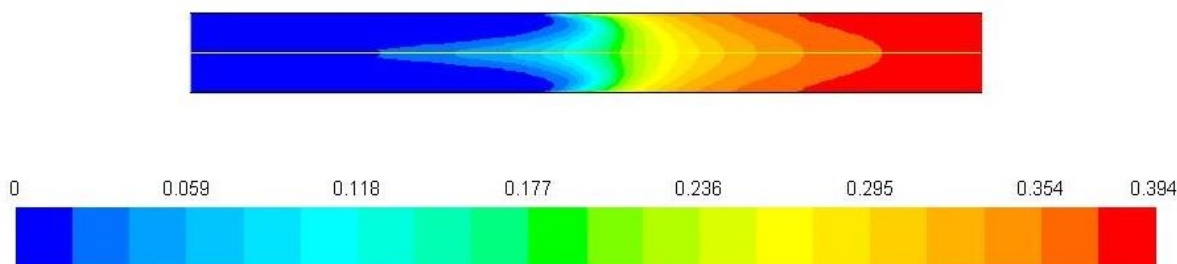


Figure 3 Mass fraction of carbon monoxide

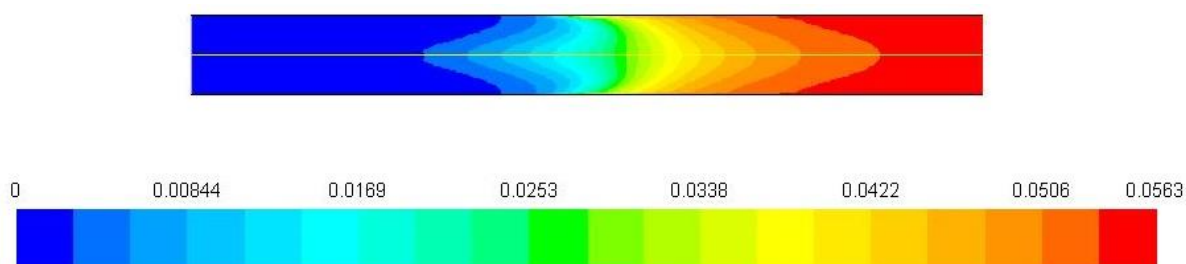


Figure 4 Mass fraction of hydrogen

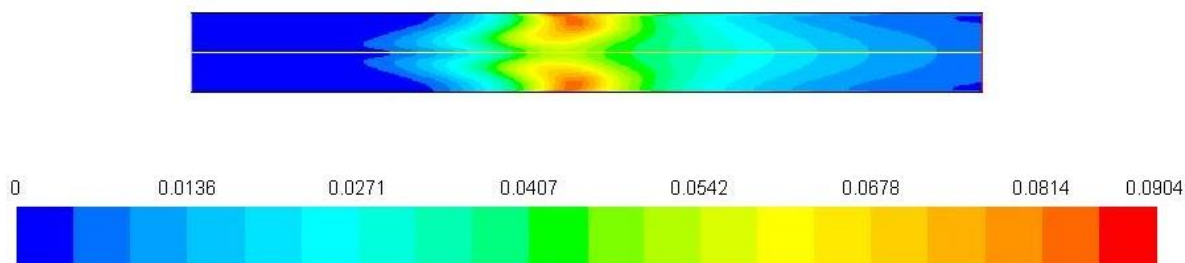


Figure 5 Mass fraction of carbon dioxide

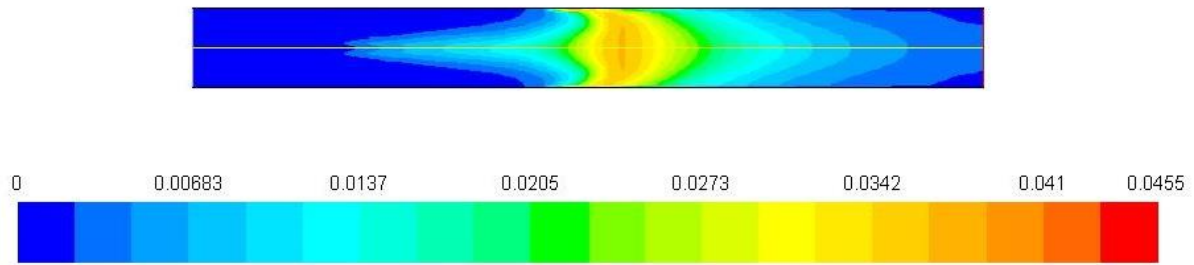


Figure 6 Mass fraction of water

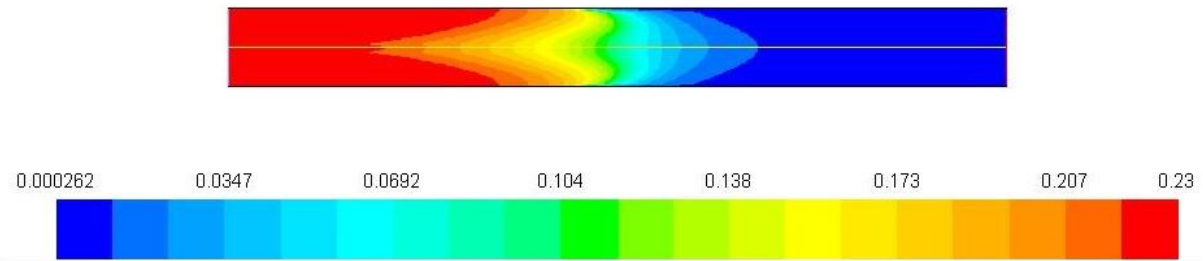


Figure 7 Mass fraction of oxygen

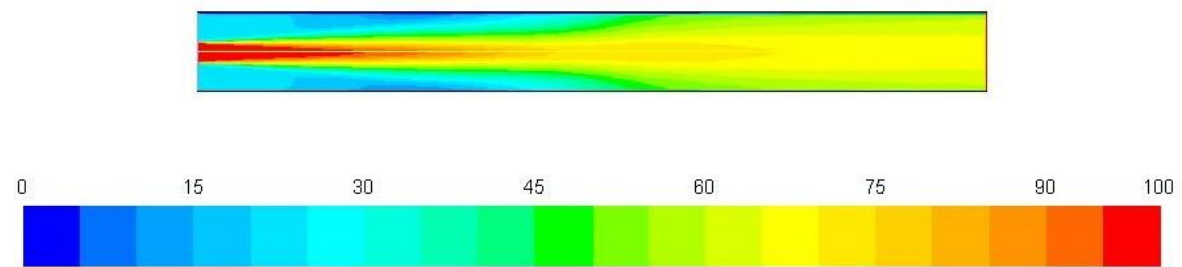


Figure 8 Velocity profile

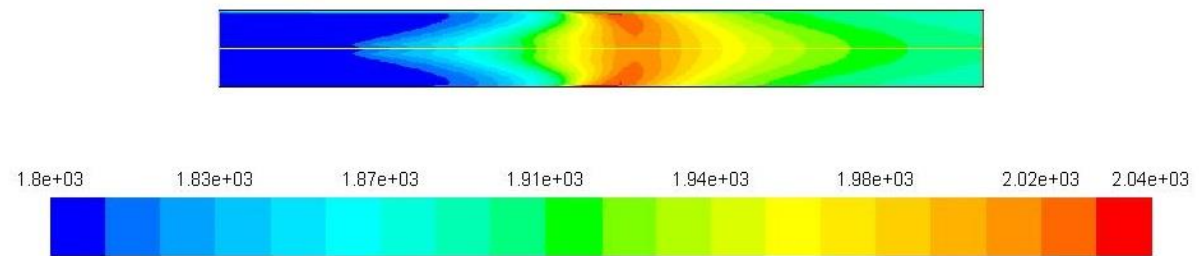


Figure 9 Temperature profile

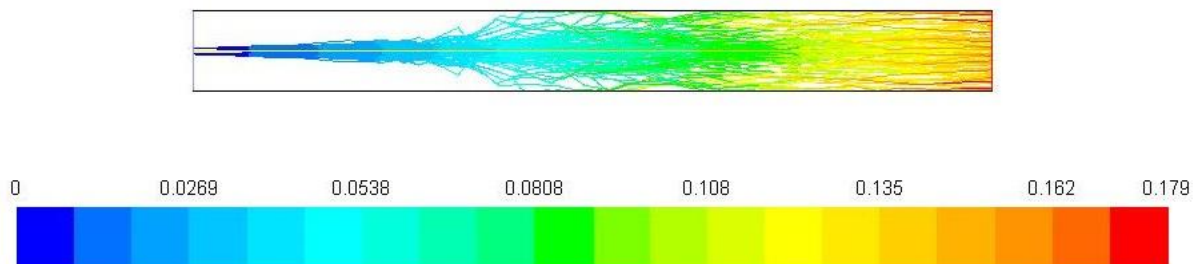


Figure 10 Residence time

Conclusion:

This CFD model has successfully been implemented for the single-stage entrained flow gasifier using the coal as an inlet feedstock. The different models are applied related to combustion, devolatilization and gasification for the syngas production. In this study, almost 13 reactions were considered, which have four surface reactions and others are gas-phase reactions. The predicted mass fraction composition of carbon dioxide, carbon monoxide, hydrogen, temperature, velocity, and residence time provides a suitable gasification trend in the gasifier. The predicted composition of the syngas behavior is following the trend reported in the literature. The heterogeneous and homogeneous reactions play a vital role in the chemical equilibrium and due to these, the syngas composition is not in equilibrium at the outlet.

REFERENCES

- Wang, M., et al., *Post-combustion CO₂ capture with chemical absorption: a state-of-the-art review*. 2011. **89**(9): p. 1609-1624.
- Higman, C. and S.J.C.r. Tam, *Advances in coal gasification, hydrogenation, and gas treating for the production of chemicals and fuels*. 2014. **114**(3): p. 1673-1708.
- Salem, A.M., et al., *The evolution and formation of tar species in a downdraft gasifier: Numerical modelling and experimental validation*. 2019. **130**: p. 105377.
- Dong, K., et al., *A novel simulation for gasification of Shenmu Coal in an entrained flow gasifier*. 2020. **160**: p. 454-464.
- Roberts, D.G. and DJFPT Harris, *A numerical model for understanding the behaviour of coals in an entrained-flow gasifier*. 2015. **134**: p. 424-440.
- Ali, D.A., et al., *Co-gasification of coal and biomass wastes in an entrained flow gasifier: Modelling, simulation and integration opportunities*. 2017. **37**: p. 126-137.
- Stein, O., et al., *Towards comprehensive coal combustion modelling for LES*. 2013. **90**(4): p. 859-884.
- Vascellari, M., et al., *From laboratory-scale experiments to industrial-scale CFD simulations of entrained flow coal gasification*. 2015. **152**: p. 58-73.
- Shahabuddin, M. and S.J.I.J.o.E.R. Bhattacharya, *Effect of reactant types (steam, CO₂ and steam+CO₂) on the gasification performance of coal using entrained flow gasifier*. 2021.
- Ma, J., SEJE Zitney, and fuels, *Computational fluid dynamic modeling of entrained-flow gasifiers with improved physical and chemical submodels*. 2012. **26**(12): p. 7195-7219.
- Abani, N. and AFJF Ghoniem, *Large eddy simulations of coal gasification in an entrained flow gasifier*. 2013. **104**: p. 664-680.
- Tufano, G., et al., *Resolved flow simulation of pulverized coal particle devolatilization and ignition in air-and O₂/CO₂-atmospheres*. 2016. **186**: p. 285-292.
- Wang, L., et al., *Numerical analysis on the influential factors of coal gasification performance in two-stage entrained flow gasifier*. 2017. **112**: p. 1601-1611.
- Cao, Z., et al., *Systems modeling, simulation and analysis for robust operations and improved design of entrained-flow pulverized coal gasifiers*. 2018. **148**: p. 941-964.
- Kartal, F., Ş. Cingisiz, and U.J.D.E.Ü.M.F.F.v.M.D. Özveren, *Investigation of Çan Coal Gasification in Entrained Flow Gasifier by using Aspen PLUS®*. **23**(67): p. 309-318.
- Westbrook, C.K., F.L.J.C.s. Dryer, and technology, *Simplified reaction mechanisms for the oxidation of hydrocarbon fuels in flames*. 1981. **27**(1-2): p. 31-43.
- Wu, Y., et al., *Effects of turbulent mixing and controlling mechanisms in an entrained flow coal gasifier*. 2010. **24**(2): p. 1170-1175.
- Hou, K. and RJCEJ Hughes, *The kinetics of methane steam reforming over a Ni/ α -Al₂O₃ catalyst*. 2001. **82**(1-3): p. 311-328.
- Nakod, PJIJCPS, *CFD modeling and validation of oxy-fired and air-fired entrained flow gasifiers*. 2013. **2**(6): p. 28-40.
- Vascellari, M., et al., *simulation of entrained flow gasification with advanced coal conversion submodels. Part I: Pyrolysis*. 2013. **113**: p. 654-669.
- Fluent, CAJAI, Cecil Township, Pennsylvania, USA, *CFD, version 17.0*. 2016.
- Chyou, Y.-P., et al., *Investigation of the gasification performance of lignite feedstock and the injection design of a cross-type two-stage gasifier*. 2013. **27**(6): p. 3110-3121.
- Chyou, Y.-P., et al., *Investigation of the Gasification Performance of Lignite Feedstock and the Injection Design of a Cross-Type Two-Stage Gasifier*. *Energy & Fuels*, 2013. **27**(6): p. 3110-3121.
- Saiful Alam, M., et al., *Study on coal gasification with soot formation in two-stage entrained-flow gasifier*. *International Journal of Energy and Environmental Engineering*, 2015. **6**(3): p. 255-265.